PURDUE UNIVERSITY

EE618: Numerical Electromagnetics

Project I

Wave propagation in parallel plate waveguide using Yee's 3D Finite-difference time-domain algorithm

A work submitted by

Chang Yang
Shuzhan Sun
Skanda Kotethota

School of Electrical and Computer Engineering
Purdue University, West Lafayette, IN 47907

Contents

1 Introduction

Maxwell's equations govern the movement of Electric field $(\vec{\boldsymbol{E}})$, Magnetic field $(\vec{\boldsymbol{M}})$, and hence the propagation of electromagnetic waves in both guided and unguided media. The Maxwell's equations in differential form are as shown in Equation (1) [1].

$$\nabla \cdot \vec{\boldsymbol{D}} = \rho_v \tag{1a}$$

$$\nabla \cdot \vec{\boldsymbol{B}} = 0 \tag{1b}$$

$$\nabla \times \vec{\boldsymbol{E}} = -\frac{\partial \vec{\boldsymbol{B}}}{\partial t} \tag{1c}$$

$$\nabla \times \vec{\boldsymbol{H}} = \frac{\partial \vec{\boldsymbol{D}}}{\partial t} + \vec{\boldsymbol{J}} \tag{1d}$$

Although Maxwell's equations have to be solved analytically to get accurate results, it may not be possible to have closed form solutions for complex structures that occur in practice. Hence, in order to solve these equations we use numerical techniques to approximate Maxwell's equations and implement them on a computer. The challenge here is to make sure that the numerical modeling is optimal for solving in terms of memory usage and run time, yet get reasonably accurate results. The three most commonly used numerical techniques for solving Maxwell's equations are: Finite-difference time-domain method (FDTD), Finite element method (FEM), and Method of moments (MoM).

1.1 Finite-difference time-domain/Yee's method

Finite-difference time-domain method is a popular technique to solve Maxwell's equations numerically in time domain. Kane S. Yee, in 1966, showed that Maxwell's equations can be replaced by a set of finite difference equations [2]. The derivatives can be represented using either forward, backward or central difference. The entire problem is split into discrete set of points in both space and time. The resulting equations, along with boundary conditions are used to determine $\vec{\boldsymbol{E}}$ and $\vec{\boldsymbol{H}}$ fields at all discretized points. The step size for space and time are related through stability criterion and can be chosen based on the accuracy required and the compute resources available.

Equations (1c) and (1d) are written in the form of scalar equations as:

$$-\frac{\partial B_x}{\partial t} = \frac{\partial E_z}{\partial y} - \frac{\partial E_y}{\partial z} \tag{2a}$$
$$-\frac{\partial B_y}{\partial t} = \frac{\partial E_x}{\partial z} - \frac{\partial E_z}{\partial x} \tag{2b}$$
$$\frac{\partial B_z}{\partial t} = \frac{\partial E_x}{\partial y} - \frac{\partial E_y}{\partial x} \tag{2c}$$
$$\frac{\partial D_x}{\partial t} = \frac{\partial H_z}{\partial y} - \frac{\partial H_y}{\partial z} - J_x \tag{2d}$$
$$\frac{\partial D_y}{\partial t} = \frac{\partial H_x}{\partial z} - \frac{\partial H_z}{\partial x} - J_y \tag{2e}$$
$$\frac{\partial D_z}{\partial t} = \frac{\partial H_y}{\partial x} - \frac{\partial H_x}{\partial y} - J_z \tag{2f}$$

A given space grid point is written with subscripts i, j, k such that $x = i\Delta x$, $y = j\Delta y$ and $z = k\Delta z$ respectively. Time index is represented with l to denote $t = l\Delta t$. The Equations (2a)-(2f) are discretized in both space and time to give:

$$\begin{aligned}\frac{\mu_{i,j+\frac{1}{2},k+\frac{1}{2}}(H^{l+\frac{1}{2}}_{x_{i,j+\frac{1}{2},k+\frac{1}{2}}} - H^{l-\frac{1}{2}}_{x_{i,j+\frac{1}{2},k+\frac{1}{2}}})}{\Delta t} &= \frac{(E^{l}_{y_{i,j+\frac{1}{2},k+1}} - E^{l}_{y_{i,j+\frac{1}{2},k}})}{\Delta z} \\ &\quad - \frac{(E^{l}_{z_{i,j+1,k+\frac{1}{2}}} - E^{l}_{z_{i,j,k+\frac{1}{2}}})}{\Delta y}\end{aligned} \tag{3a}$$

$$\begin{aligned}\frac{\epsilon_{i+\frac{1}{2},j,k}(E^{l}_{x_{i+\frac{1}{2},j,k}} - E^{l-1}_{x_{i+\frac{1}{2},j,k}})}{\Delta t} &= \frac{(H^{l-\frac{1}{2}}_{z_{i+\frac{1}{2},j+\frac{1}{2},k}} - H^{l-\frac{1}{2}}_{z_{i+\frac{1}{2},j-\frac{1}{2},k}})}{\Delta y} \\ &\quad - \frac{(H^{l-\frac{1}{2}}_{y_{i+\frac{1}{2},j,k+\frac{1}{2}}} - H^{l-\frac{1}{2}}_{y_{i+\frac{1}{2},j,k-\frac{1}{2}}})}{\Delta z} - J^{l-\frac{1}{2}}_{x_{i+\frac{1}{2},j,k}}\end{aligned} \tag{3b}$$

The other equations, (2b)-(2c) and (2e)-(2f) are discretized similarly. $\vec{\boldsymbol{E}}$ and $\vec{\boldsymbol{H}}$ field components in equations (3a) and (3b) when represented in space appear as shown in Figure 1. All components of $\vec{\boldsymbol{E}}$ field lie on the center of every edge, while all $\vec{\boldsymbol{H}}$ field components lie on the center of each face of the cube.

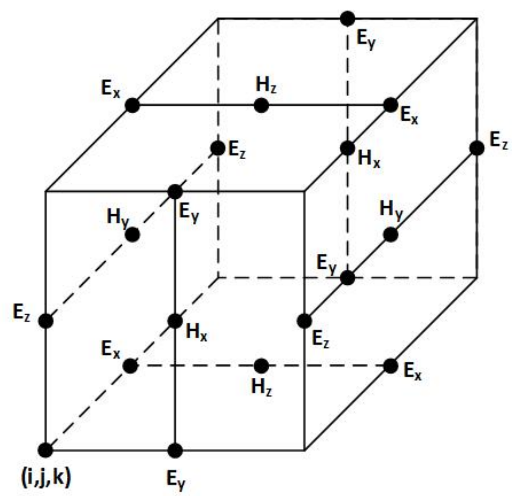

Figure 1: Representation of $\vec{\boldsymbol{E}}$ and $\vec{\boldsymbol{H}}$ components in space.

2 Parallel plate waveguide

A waveguide is a structure used in microwave communication for guiding electromagnetic waves. A parallel plate waveguide consists of two metal plates that are separated by a distance d as shown in Figure 2. This configuration allows propagation of EM waves in all modes, i.e., Transverse Electromagnetic (TEM), Transverse Electric (TE), and Transverse Magnetic (TM) mode [3].

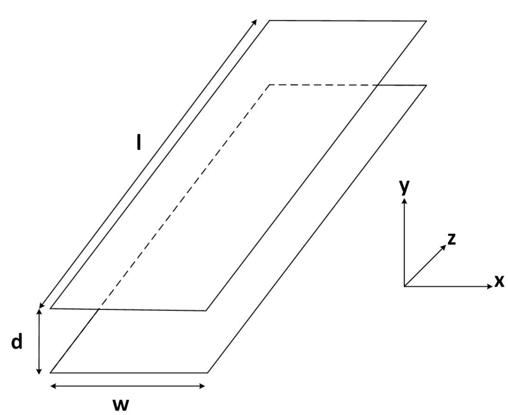

Figure 2: A parallel plate waveguide.

2.1 Theoretical Analysis

Consider a parallel plate waveguide shown in Figure 2. It is made of two metallic plates of length l that are assumed to be perfectly conducting and filled with a lossless dielectric having permitivity ϵ and permeability μ. Let w and d be the width and distance between the plates respectively. Let the wave propagate in $+z$ direction. The analytical results for various modes of propagation along the waveguide has been presented in the following section.

2.1.1 Transverse Magnetic (TM) mode

Transverse Magnetic mode is characterized by a magnetic field whose component along the direction of propagation is zero, and electric field having a non-zero component along the direction of propagation, i.e, $H_z = 0$ and $E_z \neq 0$, for a wave propagating in $+z$ direction. According to [3], the final results for $\vec{\boldsymbol{E}}$ and $\vec{\boldsymbol{H}}$ field components inside parallel plate waveguide can be written in phasor form as:

$$E_y = \frac{-j\beta}{k_c} A_n \cos \frac{n\pi y}{d} e^{-j\beta z} \tag{4a}$$

$$E_z = A_n \sin \frac{n\pi y}{d} e^{-j\beta z} \tag{4b}$$

$$H_x = \frac{j\omega\epsilon}{k_c} A_n \cos \frac{n\pi y}{d} e^{-j\beta z} \tag{4c}$$

$$E_x = H_y = H_z = 0 \tag{4d}$$

In the above equations, A_n denotes the amplitude of n^{th} mode. k_c is the cut-off wave number, β is the propagation constant of the wave, and k is the wave number.

$$k_c = \frac{n\pi}{d} \tag{5}$$

$$\beta = \sqrt{k^2 - k_c^2} \tag{6}$$

$$k = \omega\sqrt{\mu\epsilon} \tag{7}$$

From the above equations, it is evident that only the waves with frequencies satisfying the condition $k > k_c$ will propagate inside the parallel plate waveguide.

2.1.2 Transverse Electric (TE) mode

Transverse Electric mode is characterized by an electric field whose component along the direction of propagation is zero, and magnetic field having a non-zero component along the direction of propagation, i.e, $E_z = 0$ and $H_z \neq 0$, , for a wave propagating in $+z$ direction. The final results of $\vec{\boldsymbol{E}}$ and $\vec{\boldsymbol{H}}$ field components inside parallel plate waveguide in TE mode can be written in phasor form as [3]:

$$E_x = \frac{j\omega\mu}{k_c} B_n \sin\frac{n\pi y}{d} e^{-j\beta z} \tag{8a}$$

$$H_y = \frac{j\beta}{k_c} B_n \sin\frac{n\pi y}{d} e^{-j\beta z} \tag{8b}$$

$$H_z = B_n \cos\frac{n\pi y}{d} e^{-j\beta z} \tag{8c}$$

$$H_x = E_y = E_z = 0 \tag{8d}$$

where, B_n is the amplitude of the n^{th} mode. k_c, β, and k are as shown in equations (5)-(7). Similar to the TM mode case, only those frequencies that satisfy the condition $k > k_c$ can propagate along the parallel plate waveguide.

2.2 FDTD Implementation

The equations in (3) along with boundary/initial conditions are solved at each time step to give all the $\vec{\boldsymbol{E}}$ and $\vec{\boldsymbol{H}}$ field components at all discretized points within the parallel plate waveguide. The boundary conditions are considered as follows:

1. The top and bottom metallic plates are assumed to be perfect electric conductors. Hence, the tangential $\vec{\boldsymbol{E}}$ field and normal $\vec{\boldsymbol{H}}$ field on the metallic plates are considered to be equal to 0.

2. The side boundaries are considered to be perfect magnetic conductors. This implies that the tangential $\vec{\boldsymbol{H}}$ field and the normal $\vec{\boldsymbol{E}}$ field on the side walls are both equal to 0.

3. The values of $\vec{\boldsymbol{E}}$ and $\vec{\boldsymbol{H}}$ field components in front (input) and the back (output) sides are given the values from the analytical equations illustrated in Section 2.1.

The formulation of FDTD equations and subsequent determination of field components is done using MATLAB 2017. A Graphical User Interface (GUI) has been created that allows the user to enter the physical properties of the parallel plate waveguide structure, the mode of propagation and the frequency of wave propagation. The output of the simulation is a graph showing the time variation of the field component along the direction of wave propagation, i.e, E_y for TM mode and H_y for TE mode (for wave propagating along $+y$ direction) using both FDTD implementation and analytical result. The third figure shows the field variation in the yz plane highlighting the propagation of wave along $+y$ direction. A screenshot of the GUI is presented in Figure 3.
For convenience, the wave propagation for FDTD implementation in MATLAB is assumed to be in $+y$ direction, plate separation in z direction and plate width along x direction.

3 Interpretation of results

The following are some of the observations that were made from the FDTD implementation of parallel plate waveguide:

1. When the ratio of plate width to plate separation, $\frac{w}{d}$, is very small, the perfect magnetic conductor (PMC) boundary on the sides does not behave like a perfect absorbing boundary. As a result, reflection will be significant and the results do not match will the analytical results. Hence, the ratio was made small by considering a small value of d, in turn making the problem close to the infinitely-large waveguide case.

2. When all the field components were initialized to 0, it was observed that the FDTD results did not correlate with the analytical result in Section 2.1. This can be attributed to the fact that the reflections from PMC boundary get accumulated and along with the numerical error cause to deviate from the analytical result for which dimensions were assumed to be infinite. This is illustrated in Figure 4. Figure 4d provides a graphical illustration where the fields inside the waveguide gradually increase from 0. The problem due to this was fixed by taking the initial condition at all points as analytical values and the results are presented in Figure 5.

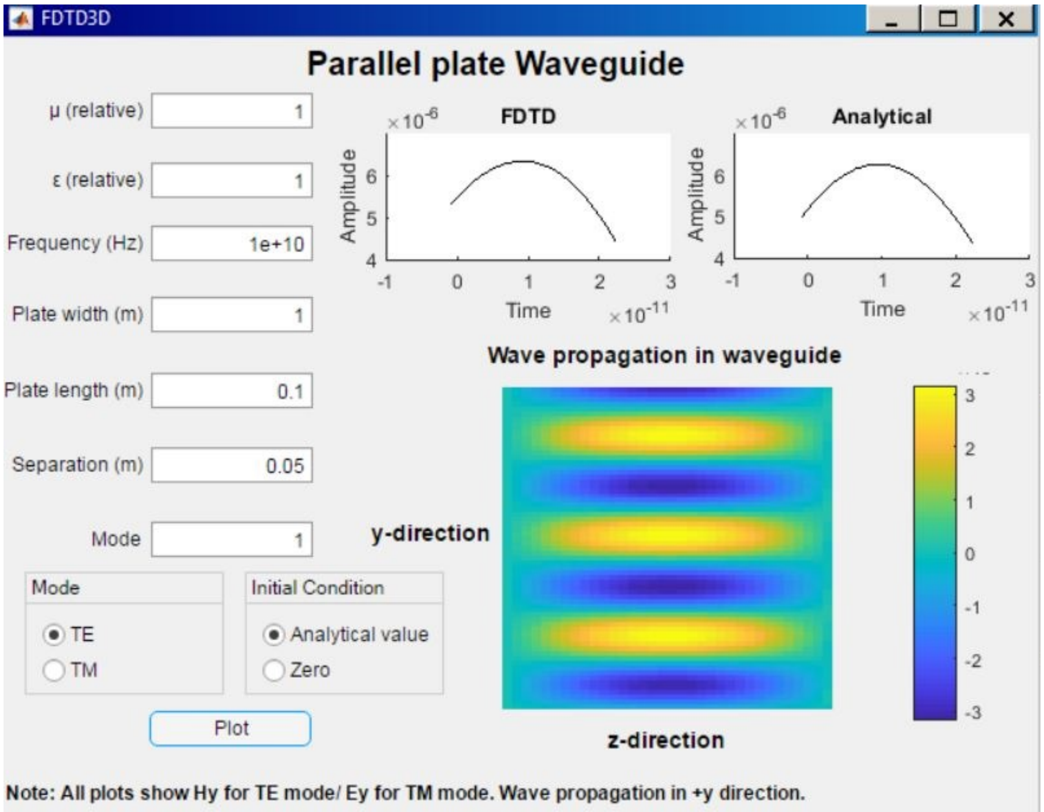

Figure 3: An interactive Graphical User Interface (GUI) for the analysis of wave propagation inside parallel plate waveguide.

3. Figure 4c and Figure 5c show the relative error between the observed and analytical results for two different cases. The error can be interpreted as arising due to the phase difference between the two results (Phase error). One of the ways the phase error could be mitigated is by using a lower value of the grid size in the direction of wave propagation, which is determined by the minimum value of signal wavelength (or maximum frequency).

4 Conclusion

The results from FDTD implementation of a parallel plate waveguide closely match with the analytical results when the initial conditions are appropri-

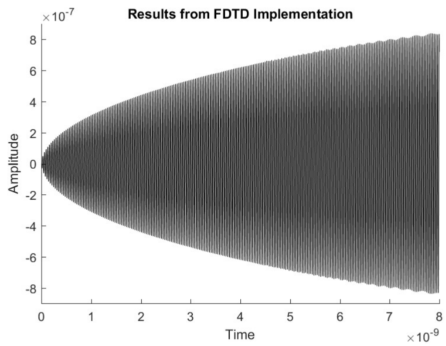

(a) FDTD Implementation

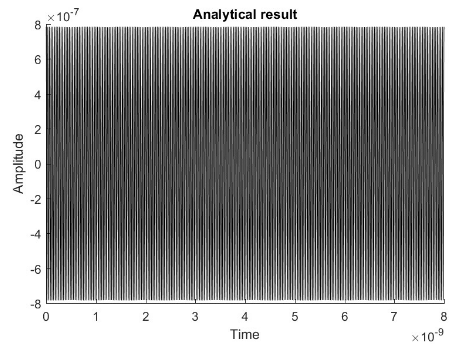

(b) Analytical result

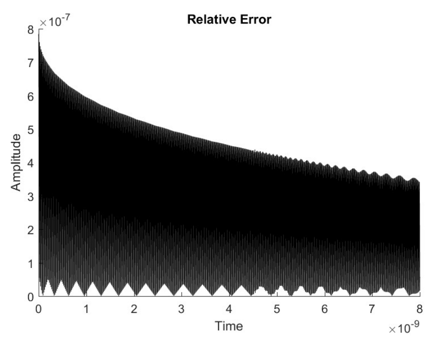

(c) Relative error

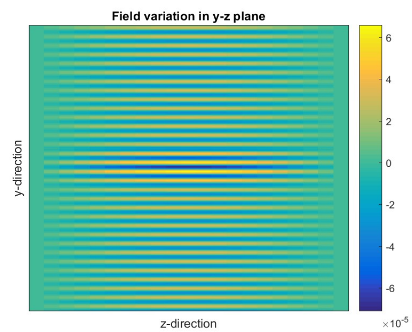

(d) Field variation in y-z plane

Figure 4: TE mode: Variation of H_y with time inside the parallel plate waveguide, when $\vec{\boldsymbol{E}}$ and $\vec{\boldsymbol{H}}$ are initialized with zero (wave along $+y$ direction).

ately taken. A GUI was created that allowed the user to enter physical dimensions of the structure and the mode of propagation. Due to the unavailability of commercial EM modeling tools, the FDTD results could not be compared with other numerical techniques. The advantage of using FDTD method is that it is very straightforward to implement it even for complex structures, since it does not involve formulation of the integral equation. The results from FDTD analysis can be made more accurate by choosing a finer step-size depending on the availability of the compute resources.

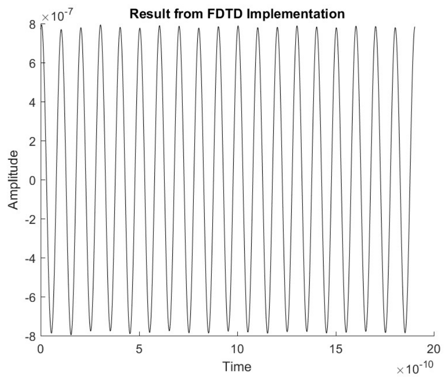

(a) FDTD Implementation

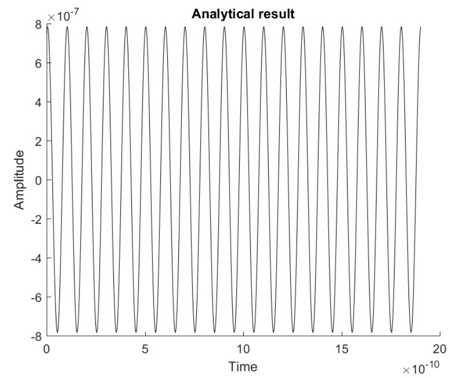

(b) Analytical result

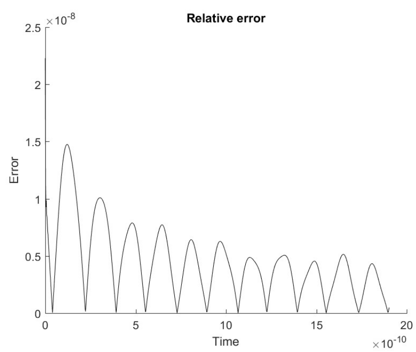

(c) Relative error

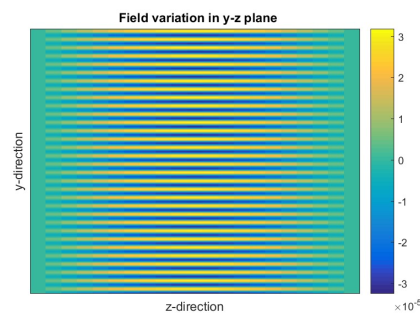

(d) Field variation in y-z plane

Figure 5: TE mode: Variation of H_y with time, inside the parallel plate waveguide, when $\vec{\boldsymbol{E}}$ and $\vec{\boldsymbol{H}}$ are initialized with analytical value (wave along $+y$ direction).

References

[1] J.-M. Jin, *Theory and Computation of Electromagnetic Fields, 2nd Edition.* John Wiley & Sons, 2015.

[2] K. Yee, "Numerical solution of initial boundary value problems involving maxwell's equations in isotropic media," *IEEE Transactions on Antennas and Propagation*, vol. 14, no. 3, pp. 302–307, May 1966.

[3] D. M. Pozar, *Microwave engineering.* Wiley, 2012.